Characterization, geostatistical modeling and health risk assessment of potentially toxic elements in groundwater resources of northeastern Iran

Joodavi, Ata ; Aghlmand, Reza; Podgorski, Joel ; Dehbandi, Reza ; Abbasi, Ali

DOI
10.1016/j.ejrh.2021.100885

Publication date
2021

Document Version
Final published version

Published in
Journal of Hydrology: Regional Studies

Journal of Hydrology: Regional Studies 37 (2021) 100885

Contents lists available at ScienceDirect

Journal of Hydrology: Regional Studies

journal homepage: www.elsevier.com/locate/ejrh

Characterization, geostatistical modeling and health risk assessment of potentially toxic elements in groundwater resources of northeastern Iran

Ata Joodavi [a], Reza Aghlmand [b], Joel Podgorski [c], Reza Dehbandi [d], Ali Abbasi [b,e,*]

[a] Department of Water Engineering, Kashmar Higher Education Institute, Kashmar, Iran
[b] Department of Civil Engineering, Faculty of Engineering, Ferdowsi University of Mashhad, Mashhad, Iran
[c] Eawag, Swiss Federal Institute of Aquatic Science and Technology, Department Water Resources and Drinking Water, Dübendorf, Switzerland
[d] Department of Environmental Health, Health Sciences Research Center, Faculty of Health, Mazandaran University of Medical Sciences, Sari, Iran
[e] Faculty of Civil Engineering and Geosciences, Water Resources Section, Delft University of Technology, Stevinweg 1, Delft, 2628 CN, The Netherlands

ARTICLE INFO

Keywords:
Groundwater quality
Health risk assessment
Random forest modelling
Toxic elements
Iran

ABSTRACT

Study region: Northeastern Iran.
Study focus: In northeastern Iran, water needed for municipal and agricultural activities mainly comes from groundwater resources. However, it is subject to substantial anthropogenic and geogenic contamination. We characterize the sources of groundwater contamination by employing an integrated approach that can be applied to the identification of large-scale contamination sources in other regions. An existing dataset of georeferenced water quality parameters from 676 locations in northeast of Iran was analyzed to investigate the geochemical properties of groundwater. Gridding of the parameters graphically illustrates the areas affected by high concentrations of As, Cl^-, Cr, Fe, Mg^{2+}, Na^+, NO_3^-, Se, and SO_4^{2-}. We then identified potential anthropogenic and geogenic contamination sources by employing random forest (RF) regression modeling.
New hydrological insights for the region: Random forest (RF) models show that the major ions, As, Cr, Fe, and Se content of groundwater are mainly determined by geology in the study area. Modeling also links groundwater NO_3^- contamination with sewage discharge into aquifers as well as the application of nitrogenous and animal-waste fertilizers. Areas of high salinity result from evaporate deposits and irrigation return flow. Medium to high non-carcinogenic health risk is found in areas with high concentrations of geogenic As and Cr in groundwater. Our approach can be applied elsewhere to analyze regional groundwater quality and associated health risks as well as identify potential sources of contamination.

1. Introduction

Many parts of Iran, like other arid/semi-arid regions, rely on groundwater to satisfy its drinking, agricultural and industrial water

* Corresponding author at: Department of Civil Engineering, Faculty of Engineering, Ferdowsi University of Mashhad, Mashhad, Iran.
E-mail addresses: atajoodavi@kashmar.ac.ir, atajoodavi@gmail.com (A. Joodavi), rezaaghlmandcivil@gmail.com (R. Aghlmand), joel.podgorski@eawag.ch (J. Podgorski), rezadehbandi65@gmail.com (R. Dehbandi), aabbasi@um.ac.ir, a.abbasi@tudelft.nl (A. Abbasi).

https://doi.org/10.1016/j.ejrh.2021.100885
Received 17 January 2021; Received in revised form 27 July 2021; Accepted 31 July 2021
Available online 6 August 2021

needs (Joodavi et al., 2015; Ashraf et al., 2021). Therefore, poor groundwater quality/groundwater pollution threatens water and food security in Iran. The chemical constituents of groundwater are determined mainly by the physical and chemical properties of an aquifer's saturated and unsaturated zones, residence time and recharge type (Khanoranga and Khalid, 2019). The geochemical conditions of an aquifer can result in high concentrations of various elements that are detrimental for human health such as As, Cd, Cr and F (Appelo and Postma, 2005). Anthropogenic activities can also introduce various pollutants of ions and trace metals to groundwater, for example through agricultural and industrial activities as well as human settlements (Barbieri et al., 2019; Ricolfi et al., 2020).

The presence of different potentially toxic elements (PTEs) in groundwater originating from geological formations and human activities is reported in some of Iran's sub-basins (Baghvand et al., 2010; Amiri et al., 2015; Dehbandi et al., 2017; Rezaei et al., 2018; Dehbandi et al., 2019; Hamidian et al., 2019; Heydarirad et al., 2019; Qasemi et al., 2019; Zendehbad et al., 2019; Sohrabi et al., 2020; Amiri et al., 2021a, b)

Most groundwater quality studies use geochemical methods and approaches to interpret geochemical reactions along groundwater flow paths and to recognize geochemical patterns in an aquifer or a watershed (local-scale studies). However, identifying both the anthropogenic and natural sources of PTEs in groundwater can be challenging in large-scale studies of broad geographical areas where there are different geological and hydrogeological conditions and large gaps in testing locations. As a way to help resolve this, geostatistical models such as logistic regression and random forest have been used to relate various environmental parameters to contaminant concentrations in groundwater and allow to create the groundwater contamination hazard maps (Bretzler et al., 2017; Podgorski and Berg, 2020; Wu et al., 2020).

This study provides a new application of geostatistical models for contamination source identification in groundwater resources through considering multiple parameters (salinity, nitrate and toxic elements) and different pollution sources.

In this paper, we present a combined approach in the large-scale identification of the sources of major ions and toxic elements in groundwater by applying random forest modeling of Razavi Khorasan province, Iran. We first describe our statistical analysis and graphical representation of water chemistry to determine ionic relationships in groundwater. We then investigate the spatial distribution of major and toxic elements and identify possible sources of groundwater contamination. Random forest modeling is then used to find relationships between contamination factors and the concentrations of toxic elements. Finally, we assess the health-risk of drinking groundwater. The findings help to understand water pollution drivers, promote stakeholder involvement, strategically plan for drinking water pollution prevention and manage health threats.

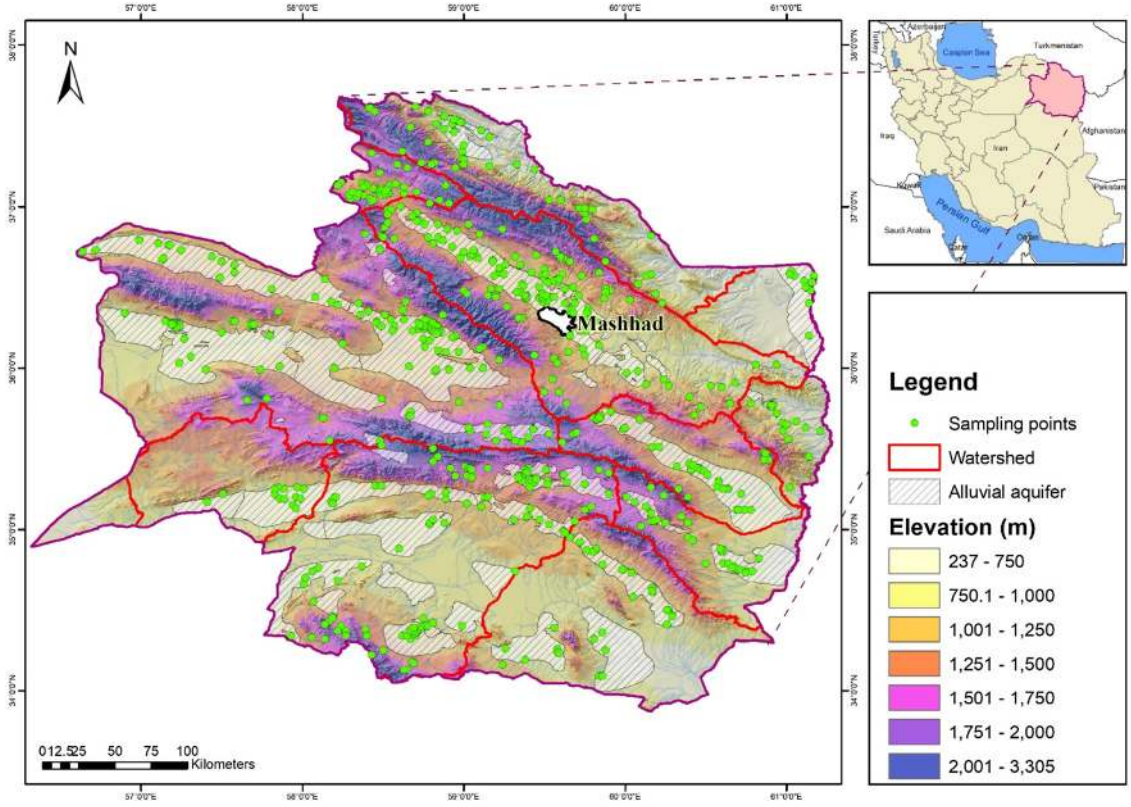

Fig. 1. Groundwater sampling points and topography within the study area of Razavi Khorasan province, Iran.

2. Materials and methods

2.1. Study area

Razavi Khorasan province, located in the northeast of Iran, has a total area of 129,043 km^2 and a population of 6,434,501 (Statistical Center of Iran, 2019). Its climate is arid to semi-arid with rainfall of 209.5 mm/year and mean temperature of 15.9 °C. About 87 % of the water used in Razavi Khorasan province (5,318 MCM) comes from groundwater that is extracted predominantly from alluvial aquifers by 23,727 wells with an average depth of 76 m and an average flow rate of 11.2 L/s. About 86 % of the groundwater withdrawn is used for agriculture, with 7% going to cities and towns used for drinking purposes (Iran Water Resources Management Company, 2019).

The geology of Razavi Khorasan includes unconsolidated Quaternary sediments, different sedimentary (sandstones, conglomerates, carbonate and evaporites), volcano-sedimentary, volcanic, intrusive, and metamorphic rocks and ophiolite series. Deposits of iron, copper, lead, zinc, chromite, aluminum, gold, arsenic, calcite, dolomite and rock salt are also found (Ghorbani, 2013).

The Quaternary sediments are mainly found in alluvial fans and plains and host alluvial aquifers (Fig. 1), which are the main source of fresh water in the study area. The water table depth in the alluvial aquifers varies between 246 m close to foothills to less than five meters in the lower-elevation parts of watersheds with an average of 63 m (Iran Water Resources Management Company, 2019).

2.2. Collection of groundwater geochemistry data sets

This study utilizes an existing dataset of georeferenced concentrations (n = 676) of EC, pH, major cations (Ca^{2+}, K^{+}, Mg^{2+}, Na^{+}), anions (Cl^{-}, HCO_3^{-}, NO_3^{-}, SO_4^{2-}), and trace elements (Al, As, Cr, Cu, Fe, Pb, Se, V, Zn) from public-supply deep wells (n = 610), springs (n = 48) and qanats (n = 18) (Fig. 1). The average depth of sampled wells is 108 m.

The data were collected by the Razavi Khorasan Water and Wastewater Company and the Razavi Khorasan regional water authority (2015–2018) as part of groundwater quality and pollution monitoring in the province (Joodavi, 2018). Sampling and Laboratory analysis methods are presented in the supplementary materials.

All of the measured ions and elements were gridded using the Inverse Distance Weighting (IDW) interpolation method (Hutchinson, 1989) in ArcGIS in order to display their spatial distributions. Relationships among the parameters were analyzed with descriptive statistics, correlation analyses and graphical representations (Piper diagrams and bivariate plots), which were together used to assess the basic hydrogeochemical processes and geochemical reactions.

Furthermore, the saturation states of the groundwater samples with respect to different minerals were calculated using PHREEQC (Parkhurst and Appelo, 2013). The saturation index (SI) of a mineral explains the mineral dissolution/precipitation possibility in the aquifer. $SI < 0$ indicates subsaturation (dissolution) and $SI > 0$ suggests supersaturation (precipitation) (Appelo and Postma, 2005).

2.3. Geostatistical modeling

2.3.1. Selection of target and predictor variables

Based on the geographical distributions of the dissolved ions and elements and their measured concentrations relative to WHO health-based guidelines (World Health Organization-WHO, 2017), the water quality parameters of As, Cr, EC, Fe, NO_3^{-}, and Se were selected as targets for random forest modeling. Predictor variables relating to potential anthropogenic and geogenic contamination sources were identified based on hydrogeochemical analyses as well as previous studies (Shojaat et al., 2003; Esmaeili-Vardanjani et al., 2015; Nematollahi et al., 2016; Taheri et al., 2016; Zirjanizadeh et al., 2016a; Alighardashi and Mehrani, 2017; Qasemi et al., 2018; Vesali Naseh et al., 2018; Hamidian et al., 2019; Zendehbad et al., 2019). Irrigated areas, urban areas, industrial areas, ophiolites and mafic rocks, intermediate to silicic volcanic (granitoid) rocks, carbonate rocks, marl/evaporite/loess, mineral deposits (metal ores) were considered as predictor variables. The attributes of independent variables are shown in Table 1 and the location maps are presented in the supplementary materials.

The main lithologies and metal ore locations, provided in Supplementary Fig. 1, are obtained from geological maps of Razavi Khorasan Province published at 1:250,000 scale (Korehie et al., 2016)

The locations of irrigated, urban and industrial areas were extracted from land use reports provided by Razavi Khorasan Management and Planning Organization (2019). All of the independent variables were available in raster format with province-wide

Table 1
Independent variables used in the RF model. All were available as rasters, which were ranked according to Table 2.

Variable	Source
Distance to irrigated areas	Razavi Khorasan Management and Planning Organization (2019)
Distance to urban areas	Razavi Khorasan Management and Planning Organization (2019)
Distance to industrial areas	Razavi Khorasan Management and Planning Organization (2019)
Distance to ophiolites and mafic	Korehie et al. (2016)
Distance to granitoid rocks	Korehie et al. (2016)
Distance to carbonate rocks	Korehie et al. (2016)
Distance to marl/evaporite/loess	Korehie et al. (2016)
Distance to metal ore deposits	Korehie et al. (2016)

coverage. New rasters were created with buffer zones at distances of 2.5, 5, 7.5 and 10 km around the features of interest. Each buffer distance was assigned a rank value from 1 to 5 according to Table 2.

2.3.2. Random Forest (RF) modeling

RF is an ensemble machine learning technique utilizing decision trees and can be used for classification or regression (Breiman, 2001 and Biau and Scornet, 2016). In regression problems, a continuous response variable is predicted by growing and then averaging many decision trees, which vary by utilizing different randomly selected data rows (with replacement) in each tree and different predictor variables at each branch (Tahmasebi et al., 2020).

Regression RF modelling was implemented using the Microsoft Excel add-in XLSTAT (Addinsoft, 2020). The main parameters of the RF model that must be specified are the number of variables randomly selected at each node (mtry) and the number of trees (ntree). The "mtry" value was set to p/3, in which p is the number of independent variables and "ntree" was set to 1000. The relative importance of the predictor variables in each model was assessed through the RF measure of importance, which gives the average model error when the independent-variable values are randomly sorted.

The predictive ability of the RF models was evaluated by three criteria: coefficient of determination (R^2), normalized root-mean-square error (NRMSE), and the Nash–Sutcliffe coefficient of efficiency (NSE) (Legates and McCabe, 1999), which are defined as follows:

$$NRMSE = \frac{\sqrt{{}^{1}/_{N}\sum_{i=1}^{N}(O_i - P_i)^2}}{O_{\max} - O_{\min}} \tag{1}$$

$$NSE = 1 - \frac{\sum_{i=1}^{N}(O_i - P_i)^2}{\sum_{i=1}^{N}(O_i - \overline{O})^2} \tag{2}$$

where O_i is an observed value, O_{min}, O_{max} *and* $\overline{O}$ are the minimum, maximum and average of the observed values respectively; and P_i is the model predicted value and N is the number of observed data. If a model produces values that are the same as the observations, NRMSE and NSE values are 0 and 1 respectively.

NRMSE shows the square of the differences between the predicted and the observed values in relation to the variability in the observed data. These three criteria together give insight into how well the models predict the observed data.

2.4. Non-carcinogenic health risk assessment

The health risk posed by exposure to the metal(loid)s As, Cr, Cu, Fe, Pb, Se, V, and Zn in groundwater was quantified using the hazard quotient (HQ) method of the USEPA (1999):

$$HQ = CDI/RfD \tag{3}$$

$$CDI = \frac{C \times IR}{BW} \tag{4}$$

where CDI is the dose of metal(loid) intake (mg/kg/day), *RfD* is the reference dose (mg/kg/day), which refers to the maximum acceptable dose of a toxic substance (Table 3), C is the concentration of metal(loid) (mg/L), IR is the ingestion rate of water, which was set to 3.49 for adults and 2.14 L/day for children (Tirkey et al., 2017; Radfard et al., 2019), and BW is body weight, which was taken as 70 kg for adults and 22.3 for children (Fakhri et al., 2015). In this study ingestion of contaminated groundwater was considered as the only exposure route to PTEs (Ravindra et al., 2019).

As the risk assessment is done for multiple metals and metalloids, the hazard index (HI) can be calculated from following equation (Qasemi et al., 2019; Sohrabi et al., 2020):

Table 2
Criteria used to create the ranked raster of independent variables.

Distance (km)	Rank
<2.5	5
2.5–5	4
5–7.5	3
7.5–10	2
>10	1

Table 3
Reference maximum acceptable doses (RfD) for each toxic metal(loid)s (USEPA, 2020).

Chemical Parameter	$RfD_{ingestion}$ (mg/kg/day)
As	0.0003
Cr	0.003
Cu	0.037
Fe	0.3
Pb	0.014
Se	0.005
V	0.009
Zn	0.3

$$HI = \sum_{i=1}^{n} HQ_i \quad (5)$$

An HQ or HI value greater than 1 indicates medium to high chronic health risk (Yousefi et al., 2018), as outlined in Supplementary Table 2.

3. Results

3.1. Groundwater hydrogeochemical characteristics and spatial distribution of physico-chemical parameters

Table 4 provides a statistical summary of the measured major anions, trace elements and other chemical parameters in the 676 data points along with the corresponding WHO guideline concentrations (World Health Organization-WHO, 2017). The gridded maps of these parameters are shown in Fig. 2. The ranking of major cation concentrations is generally $Na^+ > Ca^{2+} > Mg^{2+} > K^+$. The ranking among the major anions is $SO_4^{2-} > Cl^- > HCO_3-$. The measures of EC, SO_4^{2-}, Na^+, Mg^{2+}, and Cr exceed the maximum permissible limits in more than 10 % of the samples.

3.2. Factors controlling the major-ions chemistry in groundwater

Plotting the samples on a Piper diagram (Fig. 3) reveals that 50 % of the samples belongs to the Na-Cl type followed by Ca-Mg-Cl (27 %), Ca-HCO_3 (15 %), Ca-Na-HCO_3 (7 %) and Ca-Cl (2%). The Ca-Mg-HCO_3 water type is mostly found in the northern part of the province where EC values are all less than 1000 μS/cm, which is likely due to the dissolution of carbonates (Supplementary Fig. 6). The predominance of the Na-Cl water type indicates that evaporites such as halite and gypsum/anhydrite strongly affect the groundwater chemistry.

Bivariate plots of ionic constituents of studied samples are presented in Fig. 4. The ratio of (Ca^{2+}+Mg^{2+}) to total cations (Fig. 4a) for

Table 4
Summary of the measured samples. Descriptive statistics of the hydrochemical parameters measured in the 676 groundwater samples in the study area.

Category	Parameter	Unit	Mean ± STDV[1]	UPL[2]	No. of samples exceeds UPL
General	EC	μS/cm	1537.5 ± 1559.2	1500	228 (35 %)
	pH	–	7.8 ± 0.1	8.5	0
Major cations	Ca^{2+}	mg/L	59.5 ± 42.6	200	10 (1 %)
	K^+	mg/L	2.2 ± 1.4	200	0
	Mg^{2+}	mg/L	35.8 ± 23.8	50	122 (18 %)
	Na^+	mg/L	175.8 ± 130.8	200	220 (33 %)
Major anions	Cl^-	mg/L	148.5 ± 144.6	250	110 (16 %)
	HCO_3^-	mg/L	269.7 ± 68.5	500	5 (1 %)
	NO_3^-	mg/L	19.3 ± 15.7	50	18 (2.7 %)
	SO_4^{2-}	mg/L	227.3 ± 184.5	250	237 (35 %)
Trace elements	Al	μg/L	14.2 ± 5.2	200	0
	As	μg/L	3.1 ± 2	10	8 (1 %)
	Fe	μg/L	114.5 ± 108.5	300	43 (6 %)
	Pb	μg/L	2.6 ± 1.2	10	0
	Cr	μg/L	21.9 ± 26.8	50	113 (17 %)
	Cu	μg/L	6.4 ± 4	2000	0
	Se	μg/L	4.8 ± 2.8	10	30 (4 %)
	V	μg/L	12.2 ± 13.9	100	0
	Zn	μg/L	22.8 ± 38.5	3000	0

[1] Standard deviation.
[2] Upper permissible limit (WHO, 2017).

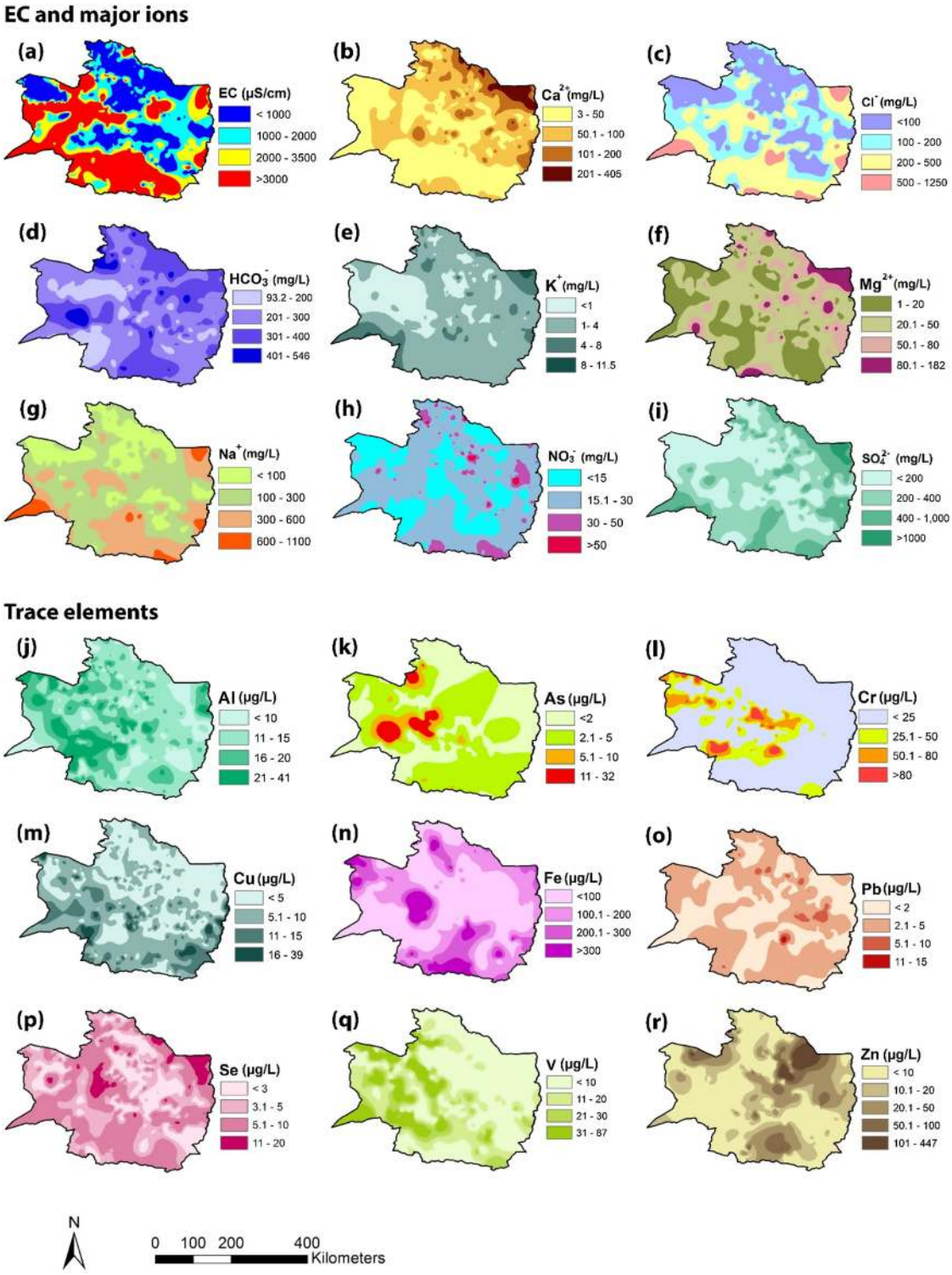

Fig. 2. Gridded maps of the hydrochemical parameters measured in groundwater in Razavi Khorasan province.

all samples is considerably less than one, which implies that other cations, such as Na^+ and K^+, are abundant in groundwater samples. The ratio of $(Ca^{2+} + Mg^{2+})$ to $(HCO_3^- + SO_4^{2-})$ of most samples is less than one (Fig. 4b), which suggests that silicate weathering affects the Ca^{2+} and Mg^{2+} chemistry (Lakshmanan et al., 2003; Dehbandi et al., 2017). The ratio of Ca^{2+} to HCO_3- for groundwater formed in dolomite and calcite aquifers is normally between 1/4 and 1/2 (Ledesma et al., 2014). However, only a few samples in Fig. 4c fall

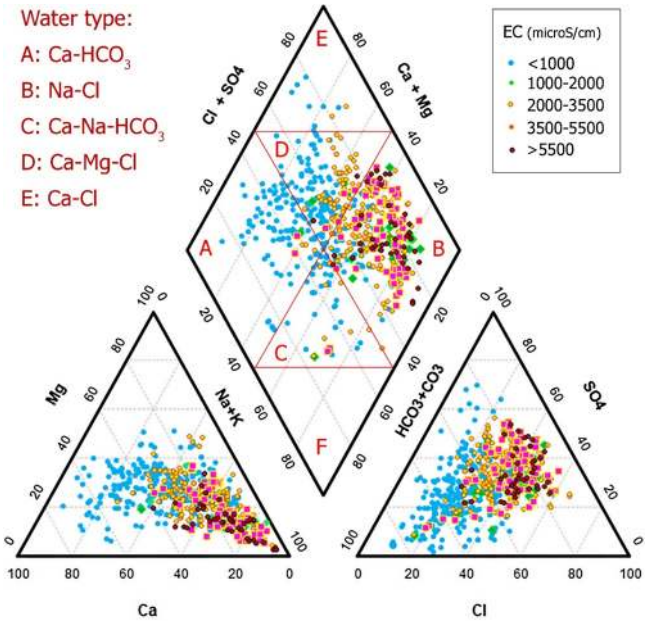

Fig. 3. Piper diagram representing the water types of the 676 groundwater samples.

between these ratios, whereas most are higher. The ratio of some samples of Ca^{2+} vs. SO_4^{2-} (Fig. 4d) is close to one, which suggests that these samples are in contact with gypsum and anhydrite (Wu et al. 2015). Examination of Fig. 4c and d suggests that Ca^{2+} is removed from water by reactions such as cation exchange. The plot of $[(Na^+ + K^+) - Cl^-]$ against $[(Ca^{2+} + Mg^{2+}) - (SO_4^{2-} + HCO_3^-)]$ (Fig. 4e) confirms the cation-exchange process with Na^+ increasing while Ca^{2+} decreases (McLean et al., 2000).

The plot of the Na^+/Cl^- ratio against Cl^- concentrations (Fig. 4f) shows that the ratio increases with decreasing salinity, with the Na^+/Cl^- ratio of the water samples ranging from 0.3 to 8.6. The majority of samples (97 %) has a molar ratio $\geq$1, which indicates that the relative abundance of sodium (Na^+) could be related to ion exchange and/or silicate weathering. This plot also shows that samples with high EC values have a molar ratio equal or close to one, which is a sign of the dissolution of evaporite minerals (Sánchez-Martos et al., 2002; Taherian and Joodavi, 2021). Furthermore, EC is significantly corelated with Na^+, Cl^-, and SO_4^{2+} (Supplementary Table 3).

The HCO_3^-/Cl^- ratio is an indicator of salinization, whereby values greater than one indicate low salinity in carbonate zones. Dissolution of evaporite minerals enriches Cl^- in groundwater, which decreases the HCO_3^-/Cl^- ratio (Fig. 4f). As seen in Fig. 4h, the water samples have a wide range of Ca^{2+}/Na^+ ratios (0.1–10), which are inversely related to salinity. A high Ca^{2+}/Na^+ molar ratio indicates that carbonate dissolution is the dominant process in the aquifer (Ayadi et al., 2018).

Moreover, the saturation index (SI) calculated by PHREEQC indicates that some groundwater samples are saturated with respect to calcite and dolomite (Fig. 5a, b, e), which confirms carbonate dissolution.

On the other hand, all samples are undersaturated with respect to gypsum and halite. SI_{gypsum} and SI_{halite} increase with TDS indicating dissolution of evaporite minerals (Fig. 5c, d). Plotting SI_{halite} versus $SI_{calcite}$ (Fig. 5f) reveals two geochemical evolution trends in the aquifer.

In relatively low salinity groundwater samples, mostly located in the northern areas and close to karst aquifers, the precipitation of Ca^{2+} and the dissolution of evaporite minerals along the groundwater flow path lead to a decrease in $SI_{calcite}$ and increase in SI_{halite} (line I in Fig. 5f). In contrast, far from carbonate formations, for example in the northeast off the study area, the dissolution of evaporites and carbonate minerals in marl and loess formations causes a simultaneous increases in $SI_{calcite}$ and SI_{halite}, EC (line ii in Fig. 5f).

3.3. *Geostatistical modelling*

Random forest (RF) regression models were used to help identify potential sources and processes of groundwater contamination. Based on the water quality assessment described above, six parameters (As, Cr, EC, Fe, NO_3^-, Se) were modeled using the variables listed in Table 1. The model results are plotted against the observations in Fig. 6, which also includes the model-performance measures (R^2, NRMSE and NSE).

The performance of the models are generally considered acceptable, as NSE and R^2 for all models are greater than 0.5 (Zhou et al., 2019). The variables' importance in each regression model indicates the strength of the relationship between a contaminant and its potential sources (Fig. 7).

The EC model confirms that high salinity is found where evaporate deposits are found (Fig. 7a and Supplementary Fig. 1) and/or

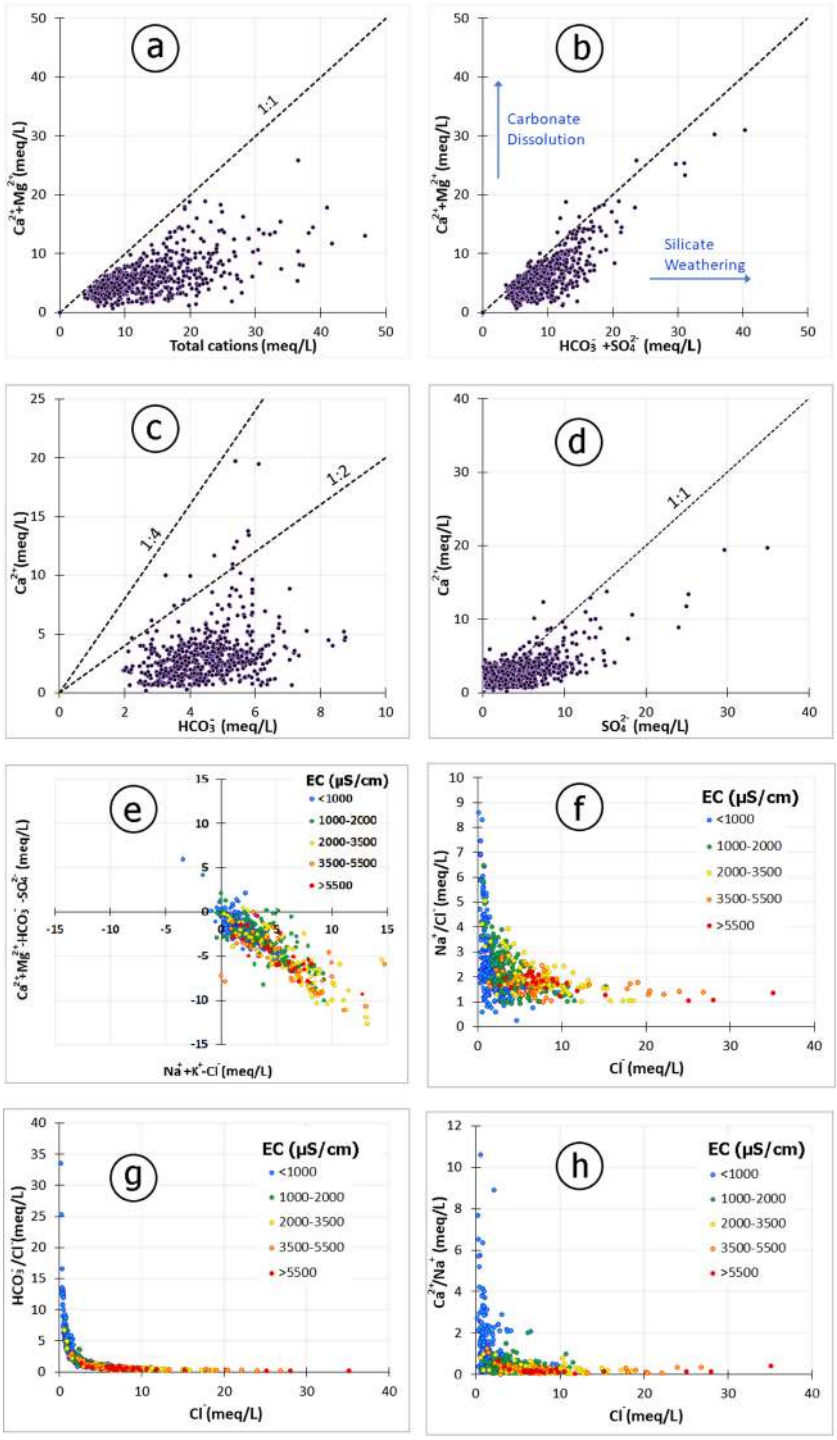

Fig. 4. Relationships between major ions showing geochemical reactions.

considerable evapotranspiration has taken place. Evaporites can exist as geological formations, such as marl, halite, gypsum, loess or salt flats (pans), and their dissolution can considerably increase groundwater salinity (Sánchez-Martos et al., 2002). Furthermore, evapotranspiration from irrigated fields can increase soil and irrigation return-flow salinity (Foster et al., 2018).

The NO_3^- model shows that nitrate in groundwater is associated primarily with urban areas followed by agricultural activities (Fig. 7c). In the study area, human sewage in cities as well as many rural areas is traditionally discharged into absorbing wells, which leads to high levels of nitrate in groundwater (Qasemi et al., 2018; Zendehbad et al., 2019). Furthermore, there are about 752,500 ha of

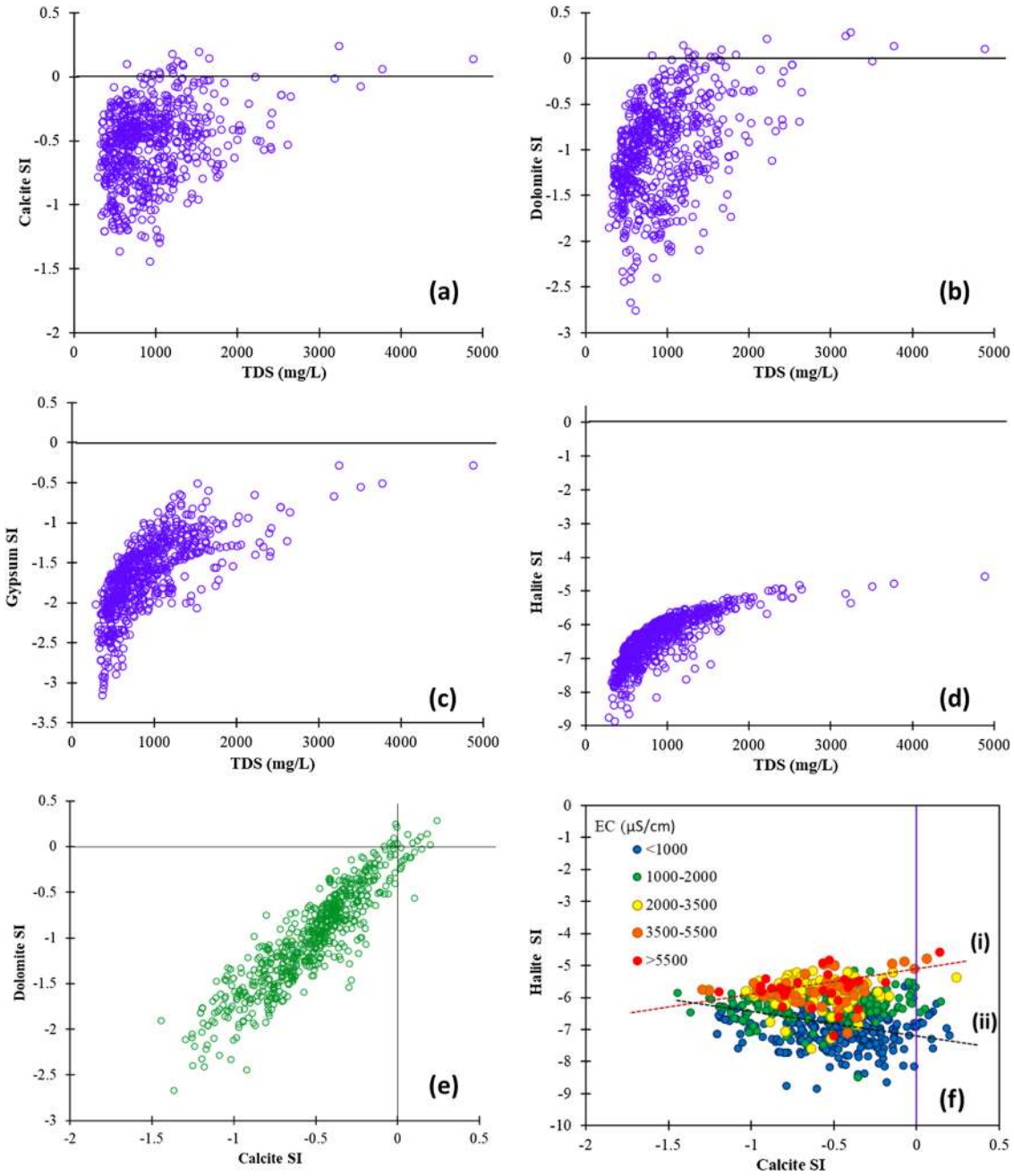

Fig. 5. Saturation Index (SI) for Calcite, Dolomite, Gypsum and Halite in groundwater samples.

irrigated agriculture in Razavi Khorasan province on which nitrogenous and animal-waste fertilizers containing high levels of nitrate are applied (Alighardashi et al., 2017).

The chromium model clearly indicates that ophiolite and ultramafic units are the main sources of chromium in groundwater. These ophiolite and ultramafic units usually consisting of peridotite, serpentinite, gabbro and chromite deposits (Shafaii Moghadam et al., 2014). Chromium is typically present as Cr(III) and Cr(VI), with Cr(VI) being very toxic and more soluble and mobile in groundwater (Coyte et al., 2019).

Cr(III) is found in minerals and can be oxidized and transformed to Cr(VI) in the existence of an oxides such as MnO_2 (Bertolo et al., 2011).

$$Cr(III) + 1.5\ MnO_2 + H_2O = HCr(VI)O_4^- + 1.5\ Mn^{2+} + H^+ \quad (6)$$

Groundwater arsenic in Razavi Khorasan is associated mainly with granitoid rocks (Fig. 7e). This is consistent with reported

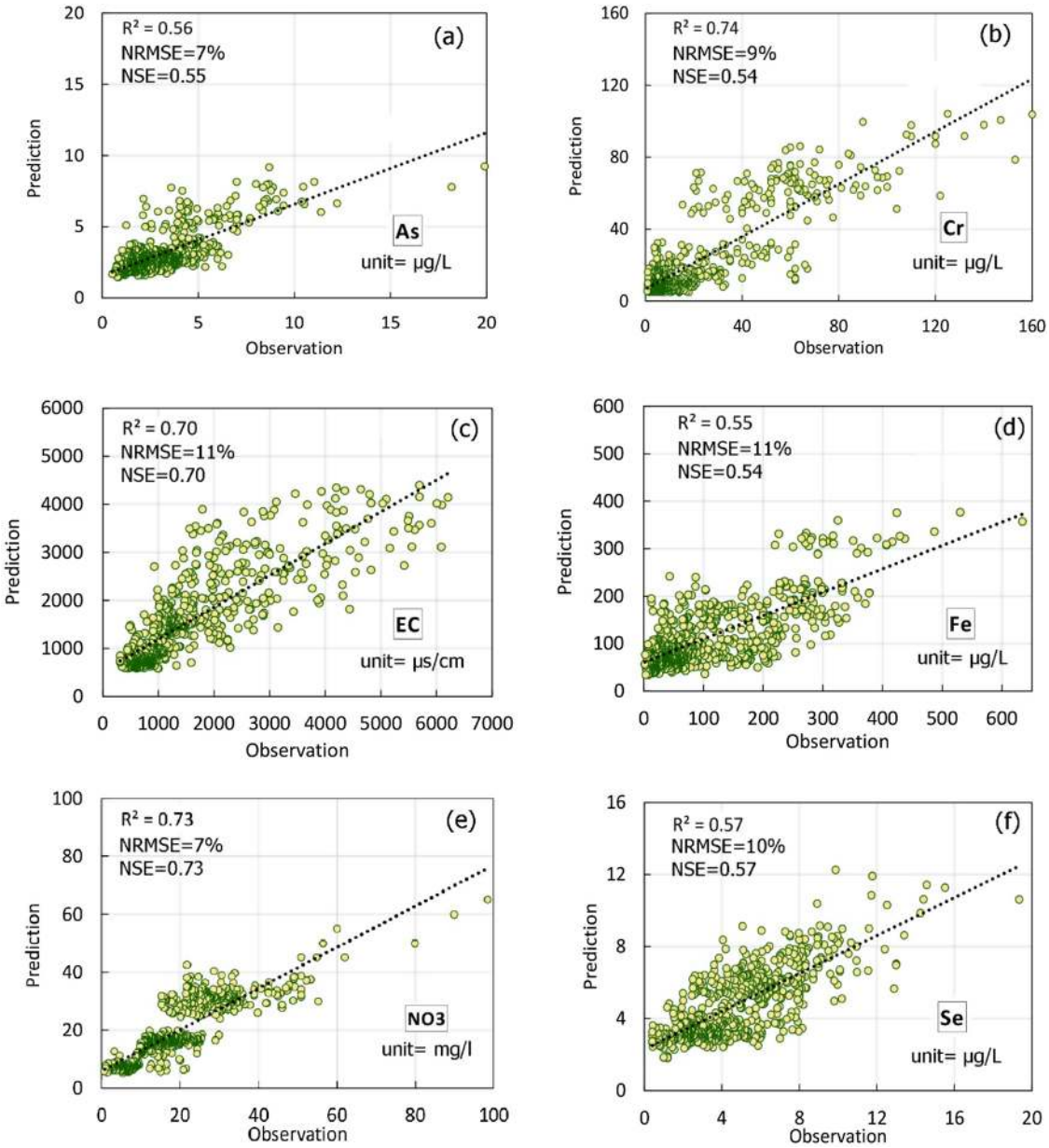

Fig. 6. Performance evaluation criteria and the plots of the predicted concentrations generated by the RF models against the observed concentrations; R^2: coefficient of determination, NRMSE: normalized root mean square error, NSE: Nash–Sutcliffe coefficient of efficiency.

geogenic arsenic-contaminated groundwater in Razavi Khorasan province (Hamidian et al., 2019), where arsenic release results from the weathering of sulfide minerals such as realgar, orpiment, and arsenopyrite in granitoid rocks (Ghasemzadeh et al., 2011; Alidadi et al., 2015; Alaminia et al., 2016; Taheri et al., 2016; Hamamipour et al., 2018).

Some possible reactions leading to the release of arsenic from sulfide minerals can be found by the following reactions (Chelsea et al., 2014):

orpiment dissolution:

$$0.5\ As_2S_3 + 3H_2O = H_3AsO_{3(aq)} + 1.5H_2S \quad (7)$$

arsenopyrite dissolution:

$$FeAsS(s) + 1.5H_2O + 2.75\ O_2(aq) = Fe_2^{2+} + H_3AsO_3\ (aq) + SO_4^{2-}\ (aq) \quad (8)$$

Fig. 7d shows that the presence of metal ore deposits is the dominant predictor of iron concentration in groundwater. Previous

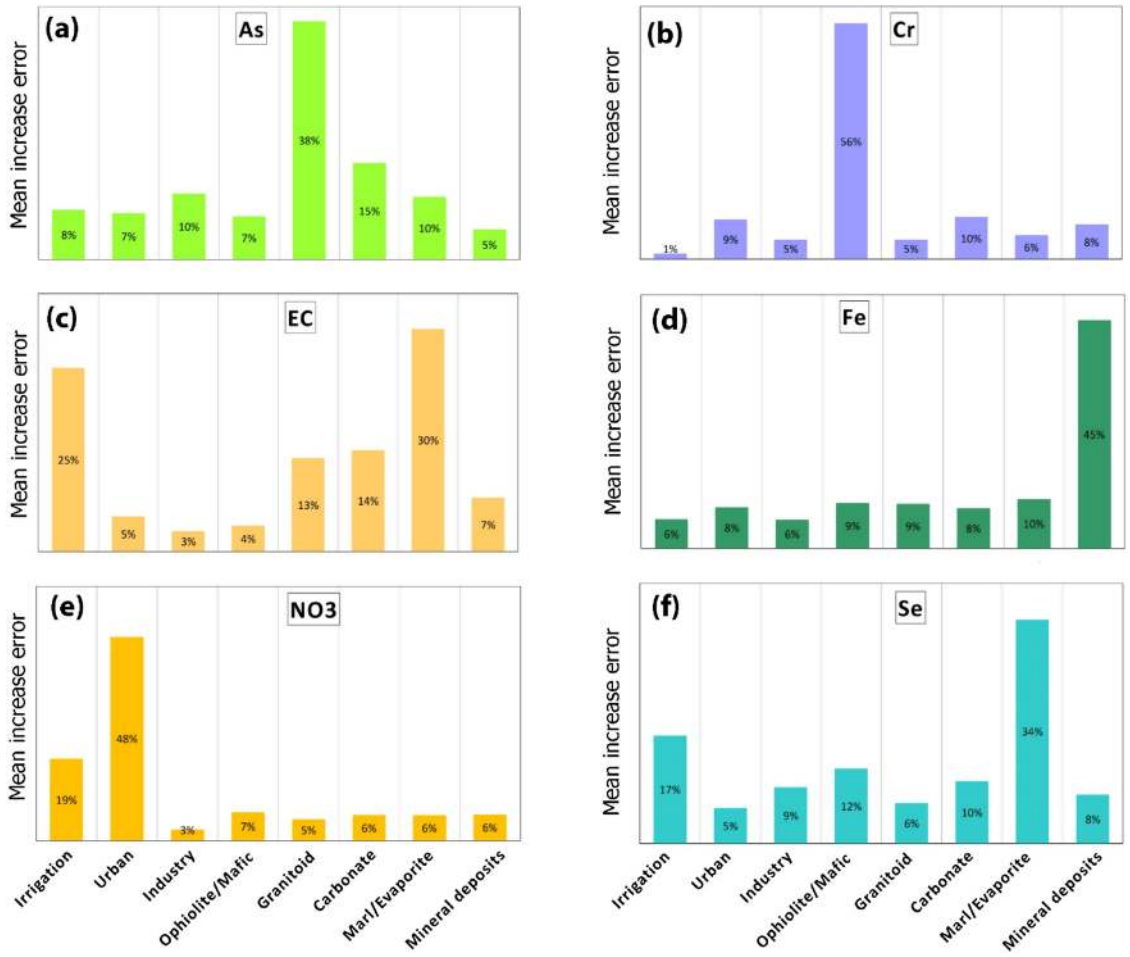

Fig. 7. Importance of the independent variables of the random forest models. The mean increase in error refers to the effect when a variable is randomly sorted.

studies indicated that iron can originate from trachyandesite and pyroclastic rocks in some parts of Razavi Khorasan province (Zirjanizadeh et al., 2016b; Taghadosi et al., 2018). Moreover, the well-known Sangan iron skarn deposit, which is located in the southeastern parts of the study area, is another well-known source of iron (Golmohammadi et al., 2015; Sepidbar et al., 2017).

The likely sources of groundwater contaminants based on the modeling results are summarized in Table 5.

3.4. Health risk assessment

A non-carcinogenic health risk assessment was conducted to estimate the probability of harmful effects of exposure to As, Cr, Cu, Fe, Pb, Se, V and Zn in groundwater used for drinking purposes.

The average hazard quotient (HQ) values indicate that As and Cr make up 53 % and 28 %, respectively, of the total non-carcinogenic risk (HI) due to groundwater constituents for the total population. HI ranges between 0.33 and 7.33 (average of 1.67) for children and between 0.13 and 3.01 (average of 0.65) for adults. Fig. 8 shows that areas with medium to high-risk values for

Table 5
Summary of main groundwater contamination sources as inferred from the random forest regression models.

Parameter	Source(s)	
As	Geology	granitoid rocks
Cr	Geology	ophiolites
EC	Geology/Agriculture	marl/evaporite/loess\groundwater-irrigated agriculture
Fe	Geology	metal ores
NO_3^-	Urban/Agriculture	waste water/fertilizer
Se	Geology	marl/evaporite/loess

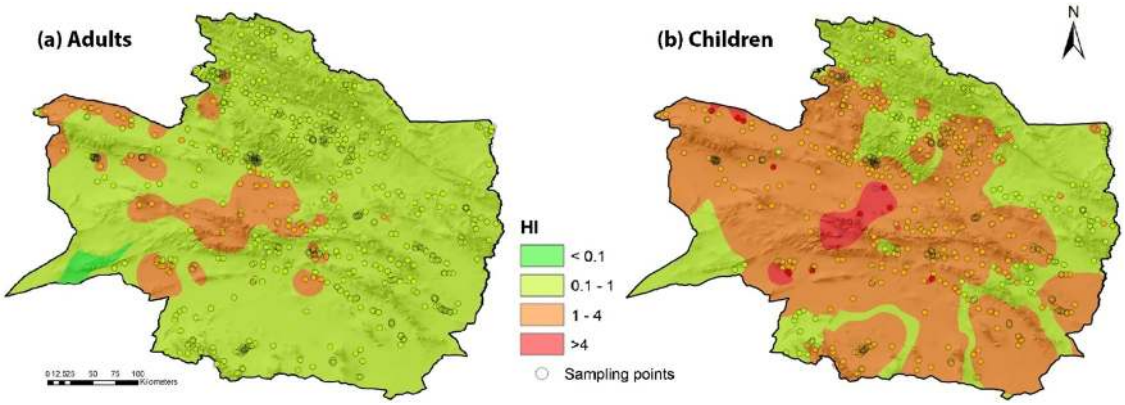

Fig. 8. Spatial distribution of non-carcinogenic hazard index (HI) for (a) adults and (b) children.

children largely coincide with zones of high As and Cr concentrations (Fig. 2).

In addition to causing adverse non-carcinogenic health effects, arsenic and chromium are categorized as carcinogenic substances (World Health Organization-WHO, 2017). The chronic consumption of As-contaminated water may cause skin, bladder or lung cancer (Polya and Middleton, 2017; World Health Organization-WHO, 2017), whereby chromium, especially Cr(VI), is known to cause DNA damage (Agency for Toxic Substances and Disease Registry (ATSDR), 2012; Wang et al., 2017).

4. Discussion

Despite there being separate alluvial aquifer systems in the study area separated by mountains, the results show that the dominant lithology of the mountains is responsible for controlling groundwater chemistry and increasing the concentration of some PTEs in groundwater, such as As, Cr, Fe and V, beyond the river-basin/aquifer boundaries. This can be conceptualized by two phenomena presented in Fig. 9.

If mountain block/front recharge exists, the chemistry of subsurface inflow directly affects the groundwater quality in alluvial aquifers (Fig. 9a) (Ajami et al., 2011; Joodavi et al., 2016). That is common in karst-alluvial aquifer systems in the northern parts of the study area where low salinity groundwater with Ca-Mg-HCO_3 water type can be found in alluvial aquifers. Moreover, it is possible that this mountain system recharge is responsible for high concentrations of arsenic in the western parts of the province where arsenic is released by weathering of sulfide minerals in granitoid rocks.

Even if the mountain block/front recharge component is not significant, the alluvial aquifers could contain particles from adjacent mountains (Fig. 9b) (Kaprara et al., 2014). The random forest model suggests that high Cr concentrations in groundwater are observed in the alluvial aquifers located not far from the ophiolitic rocks. While these rocks do not have a developed fractured storage system, the sediments of the alluvial aquifers originated from ophiolite and ultramafic units are likely the source of Cr in groundwater.

Furthermore, the geological map show that marl/evaporites are mainly found in the southern and western parts of the region. Hydrogeological studies have shown that these units form the bedrock of alluvial aquifers in these areas (Joodavi et al., 2009; Izady et al., 2015). The random forest model results confirm that groundwater resources in these areas are more saline.

The approach provided here identification of the sources of major ions and toxic elements in groundwater in regions lacking adequate monitoring programs and sampling data. Therefore, additional groundwater quality measurements and geochemical and mineralogical information as well as more information about the amount and chemistry of industrial wastewater would improve the robustness of the geostatistical models, especially in locations close to contamination sources such as industrial areas."

Another limitation of this study is that this method characterizes large-scale (macro-scale) spatial variation in the elements in groundwater. However, the chemical composition of groundwater samples may be affected by local hydrologic and hydrogeological factors. Future research will add consideration of these local factors such as residence time to accurately investigate the driving forces of groundwater quality.

5. Conclusion

Understanding the factors affecting and controlling groundwater quality is necessary to improve water security and public health through reducing water-related risks.

Although most hydrogeochemistry studies try to interpret geochemical reactions along groundwater flow paths in an aquifer or a watershed, this paper proposed an approach to identify the sources of salinity, nitrate and PTEs in groundwater in large-scale studies of broad geographical areas where there are large gaps in testing locations.

Integrated approaches of statistical analysis, conventional hydrogeochemical plots, and machine learning were employed in this study to characterize the groundwater chemistry in Razavi Khorasan province and identify likely sources of contamination. Hydrogeochemical controls on groundwater quality and human health risk from harmful elements in the province were identified from 676

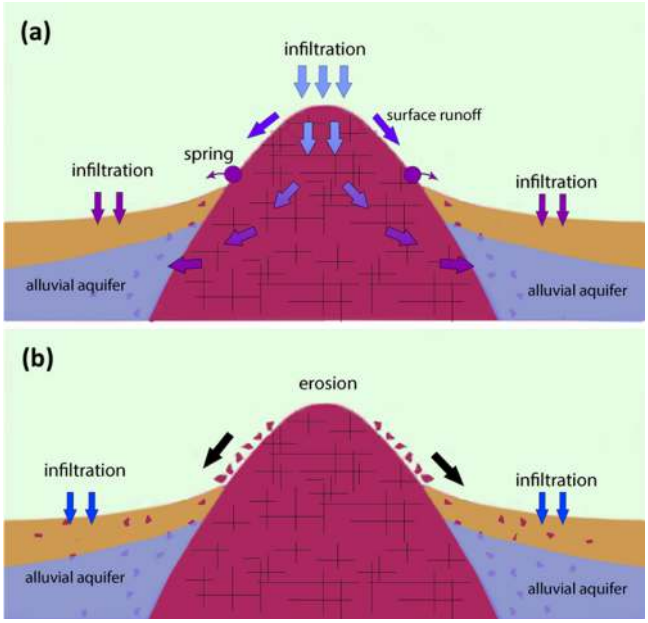

Fig. 9. Two conceptual models showing the effects of geology on groundwater quality beyond the river-basin/aquifer boundaries.

groundwater samples in the study area.

We found that the chemical composition of groundwater is determined predominantly by geology but also influenced by human activities. The Na-Cl water type along with high salinity levels in groundwater, Se and SO_4^{2-} can be related to the dissolution of salts from geological formations as well as evapotranspiration and irrigation return flow caused by groundwater-irrigated agriculture. Random forest regression modeling has also shown that high concentrations of chromium, arsenic and iron in groundwater are attributed to the presence of ophiolites, granitoid (intermediate to silicic volcanic) rocks and metal ores (formed in pyroclastic rocks and skarn deposits), respectively. Moreover, discharging sewage directly into aquifers and applying fertilizers in agricultural activities result in high levels of nitrate in groundwater. A non-carcinogenic health risk assessment of PTEs (As, Cr, Cu, Fe, Pb, Se, V, Zn) in groundwater indicates that As and Cr constitute 53 % and 28 % of the total risk, respectively.

The predictor variables used in the random forest modeling are readily available, making this integrated approach relevant for identifying potential regional groundwater contamination sources. The results can be used to develop cost-effective water quality monitoring programs for water resource planning and management in Razavi Khorasan province, Iran.

CRediT authorship contribution statement

Ata Joodavi: Conceptualization, Methodology, Writing - original draft. **Reza Aghlmand:** Data curation, Investigation. **Joel Podgorski:** Supervision, Writing - review & editing. **Reza Dehbandi:** Formal analysis, Validation. **Ali Abbasi:** Investigation, Writing - review & editing.

Declaration of Competing Interest

The authors declare that they have no known competing financial interests or personal relationships that could have appeared to influence the work reported in this paper.

Acknowledgments

This research was financially supported by Iran National Science Foundation (INSF), Grant Number 97008161 and the Swiss Agency for Development and Cooperation (project no. 7F-09963.01.01).

Appendix A. Supplementary data

Supplementary material related to this article can be found, in the online version, at doi:https://doi.org/10.1016/j.ejrh.2021.100885.

References

Addinsoft, 2020. XLSTAT Statistical and Data Analysis Solution. Boston, USA. https://www.xlstat.com.

Agency for Toxic Substances and Disease Registry (ATSDR), 2012. Toxicological Profile for Chromium. U.S. Department of Health and Human Services, Public Health Service, Atlanta, GA.

Ajami, H., Troch, P., Maddock, T., Meixner, T., Eastoe, C., 2011. Quantifying mountain block recharge by means of catchment-scale storage-discharge relationships. Water Resour. Res. 47 https://doi.org/10.1029/2010WR009598.

Alaminia, Z., Karimpour, M.H., Homam, S.M., 2016. Mineralization and trace element distribution in pyrite using EMPA in exploration drill holes from Cheshmeh Zard gold district, Khorasan Razavi Province. Iran. J. Econ. Geol. 7 (2), 203.

Alidadi, H., Ramezani, A., Davodi, M., Peiravi, R., Paydar, M., Dolatabadi, M., Rafe, S., 2015. Determination of total arsenic in water resources: a case study of Rivash in Kashmar City. J. Health Scope 4 (3). https://doi.org/10.17795/jhealthscope-25424.

Alighardashi, A., Mehrani, M.J., 2017. Survey and zoning of nitrate-contaminated groundwater in Iran. J. Mater. Environ. Sci. 8 (12), 4339–4348.

Amiri, V., Sohrabi, N., Dadgar, M.A., 2015. Evaluation of groundwater chemistry and its suitability for drinking and agricultural uses in the Lenjanat plain, central Iran. Environ. Earth Sci. 74, 6163–6176. https://doi.org/10.1007/s12665-015-4638-6.

Amiri, V., Kamrani, S., Ahmad, A., et al., 2021a. Groundwater quality evaluation using Shannon information theory and human health risk assessment in Yazd province, central plateau of Iran. Environ. Sci. Pollut. Res. 28, 1108–1130. https://doi.org/10.1007/s11356-020-10362-6.

Amiri, V., Li, P., Bhattacharya, P., et al., 2021b. Mercury pollution in the coastal Urmia aquifer in northwestern Iran: potential sources, mobility, and toxicity. Environ. Sci. Pollut. Res. 28, 17546–17562. https://doi.org/10.1007/s11356-020-11865-y.

Appelo, C., Postma, D., 2005. Geochemistry, Groundwater and Pollution, 2nd edition. Balkema, Rotterdam. https://doi.org/10.1201/9781439833544.

Ashraf, S., Nazemi, A., AghaKouchak, A., 2021. Anthropogenic drought dominates groundwater depletion in Iran. Sci. Rep. 11, 9135. https://doi.org/10.1038/s41598-021-88522-y.

Ayadi, R., Trabelsi, R., Zouari, K., et al., 2018. Hydrogeological and hydrochemical investigation of groundwater using environmental isotopes (18O, 2H, 3H, 14C) and chemical tracers: a case study of the intermediate aquifer, Sfax, southeastern Tunisia. Hydrogeol. J. 26, 983–1007. https://doi.org/10.1007/s10040-017-1702-1.

Baghvand, A., Nasrabadi, T., Nabi Bidhendi, G., Vosoogh, A., Karbassi, A., Mehrdadi, N., 2010. Groundwater quality degradation of an aquifer in Iran central desert. Desalination 260, 264–275.

Barbieri, M., Ricolfi, L., Vitale, S., et al., 2019. Assessment of groundwater quality in the buffer zone of Limpopo National Park, Gaza Province, Southern Mozambique. Environ. Sci. Pollut. Res. 26, 62–77. https://doi.org/10.1007/s11356-018-3474-0.

Bertolo, R., Bourotte, C., Hirata, R., Marcolan, L., Sracek, O., 2011. Geochemistry of natural chromium occurrence in a sandstone aquifer in Bauru Basin, São Paulo State, Brazil. Appl. Geochem. 26 (8), 1353–1363. https://doi.org/10.1016/j.apgeochem.2011.05.009.

Biau, G., Scornet, E., 2016. A random forest guided tour. TEST 25, 197–227. https://doi.org/10.1007/s11749-016-0481-7.

Breiman, L., 2001. Random forest. Mach. Learn. 45, 5–32. https://doi.org/10.1023/A:1010933404324.

Bretzler, A., et al., 2017. Groundwater arsenic contamination in Burkina Faso, West Africa: predicting and verifying regions at risk. Sci. Total Environ. https://doi.org/10.1016/j.scitotenv.2017.01.147.

Chelsea, W.N., Yang, Y.J., Schupp, D., Jun, Y.Sh., 2014. Water chemistry impacts on arsenic mobilization from arsenopyrite dissolution and secondary mineral precipitation: implications for managed aquifer recharge. Environ. Sci. Technol. 48 (8), 4395–4405. https://doi.org/10.1021/es405119q.

Coyte, R.M., McKinley, K.L., Jiang, S., Karr, J., Dwyer, G.S., Keyworth, A.J., Davis, C.C., Kondash, A.J., Vengosh, A., 2019. Occurrence and distribution of hexavalent chromium in groundwater from North Carolina, USA. Sci. Total Environ. https://doi.org/10.1016/j.scitotenv.2019.135135.

Dehbandi, R., Moore, F., Keshavarzi, B., Abbasnejad, A., 2017. Fluoride hydrogeochemistry and bioavailability in groundwater and soil of an endemic fluorosis belt, central Iran. Environ. Earth Sci. 76 (4), 177.

Dehbandi, R., Abbasnejad, A., Karimi, Z., Herath, I., Bundschuh, J., 2019. Hydrogeochemical controls on arsenic mobility in an arid inland basin, Southeast of Iran: the role of alkaline conditions and salt water intrusion. Environ. Pollut. 249, 910–922.

Esmaeili-Vardanjani, M., Rasa, I., Amiri, V., et al., 2015. Evaluation of groundwater quality and assessment of scaling potential and corrosiveness of water samples in Kadkan aquifer, Khorasan-e-Razavi Province, Iran. Environ. Monit. Assess. 187, 53. https://doi.org/10.1007/s10661-014-4261-0.

Fakhri, Y., Jafarzadeh, S., Moradi, B., et al., 2015. The non-carcinogenic risk of cadmium in bottled water in different age groups humans: Bandar Abbas City, Iran. Mater. Sociomed. 27 (Feb. (1)), 52–55. https://doi.org/10.5455/msm.2014.27.52-55.

Foster, S., Pulido-Bosch, A., Vallejos, Á., et al., 2018. Impact of irrigated agriculture on groundwater-recharge salinity: a major sustainability concern in semi-arid regions. Hydrogeol. J. 26, 2781–2791. https://doi.org/10.1007/s10040-018-1830-2.

Ghasemzadeh, F., Shafaroodi, A.A., 2011. Environmental impacts of arsenic in Cheshmeh Zard area, southwest of Neyshabour, Khorasan Razavi province. Iran. J. Crystallogr. Mineral. 19 (3), 545–556 (In Persian).

Ghorbani, M., 2013. Economic Geology of Iran, Mineral Deposits and Natural Resources of Iran. Springer Geology.

Golmohammadi, A., Karimpour, M.H., Malekzadeh Shafaroudi, A., Mazaheri, S.A., 2015. Alteration-mineralization, and radiometric ages of the source pluton at the Sangan Iron skarn deposit, Northeastern Iran. Ore Geol. Rev. 65, 545–563. https://doi.org/10.1016/j.oregeorev.2014.07.005.

Hamamipour, B., Tajeddin, H.A., Barahmand, L., 2018. Geology and mineralization of Sebandoon gold deposit, North of Bardeskan. J. Geosci. 27 (108), 155–168. https://doi.org/10.22071/gsj.2017.77437.1030.

Hamidian, A.H., Razeghi, N., Zhang, Y., Yang, M., 2019. Spatial distribution of arsenic in groundwater of Iran, a review. J. Geochem. Explor. 201, 88–98. https://doi.org/10.1016/j.gexplo.2019.03.014.

Heydarirad, L., Mosaferi, M., Pourakbar, M., et al., 2019. Groundwater salinity and quality assessment using multivariate statistical and hydrogeochemical analysis along the Urmia Lake coastal in Azarshahr plain, North West of Iran. Environ. Earth Sci. 78, 670. https://doi.org/10.1007/s12665-019-8655-8.

Hutchinson, M.F., 1989. A new procedure for gridding elevation and stream line data with automatic removal of spurious pits. J. Hydrol. 106, 211–232. https://doi.org/10.1016/0022-1694(89)90073-5.

Iran Water Resources Management Company, 2019. Iran Water Resources Management Company [Online]. Available: https://www.wrm.ir. (Accessed 23 December 2019).

Izady, A., Davary, K., Alizadeh, A., et al., 2015. Groundwater conceptualization and modeling using distributed SWAT-based recharge for the semi-arid agricultural Neishaboor plain, Iran. Hydrogeol. J. 23, 47–68. https://doi.org/10.1007/s10040-014-1219-9.

Joodavi, A., 2018. Effects of Geology on the Quality of Drinking Water Wells in Razavi Khorasan Province. Razavi Khorasan Water and Wastewater Company. In Farsi.

Joodavi, A., Zare, M., Etemadi, B., 2009. Hydrogeochemistry and sources of groundwater salinity in Feyz-Abad plane. In: Ahvaz, Iran12th Symposium of the Geological Society of Iran, 2, pp. 411–417. In Farsi.

Joodavi, A., Zare, M., Mahootchi, M., 2015. Development and application of a stochastic optimization model for groundwater management: crop pattern and conjunctive use consideration. Stochast. Environ. Res. Risk Assess. J. https://doi.org/10.1007/s00477-015-1049-x.

Joodavi, A., Zare, M., Raeisi, E., Ahmadi, M.B., 2016. A multi-compartment hydrologic model to estimate groundwater recharge in an alluvial-karst system. Arab. J. Geosci. 9, 195. https://doi.org/10.1007/s12517-015-2084-0.

Kaprara, E., Kazakis, N., Simeonidis, K., Coles, S., Zouboulis, A.I., Samaras, P., Mitrakas, M., 2014. Occurrence of Cr(VI) in drinking water of Greece and relation to the geological background. J. Hazard. Mater. 281, 2–11. https://doi.org/10.1016/j.jhazmat.2014.06.084.

Khanoranga, Khalid, S., 2019. An assessment of groundwater quality for irrigation and drinking purposes around brick kilns in three districts of Balochistan province, Pakistan, through water quality index and multivariate statistical approaches. J. Geochem. Explor. 197, 14–26. https://doi.org/10.1016/j.gexplo.2018.11.007.

Korehie, M.T., Ardebili, O., Dadashzadeh Ahari, H., Rezaei Shirzad, M., Fotovati, V., Ghalamghash, J., Kiani, T., Najafi, A., 2016. Atlas of Iran's Geology and Mineral Distribution with Maps on Scale 1:250.000. Geological Survey of Iran. In Farsi.

Lakshmanan, E., Kannan, R., Kumar, M.S., 2003. Major ion chemistry and identification of hydrogeochemical processes of ground water in a part of Kancheepuram district, Tamil Nadu, India. Environ. Geosci. 10 (4), 157–166.
Ledesma, R., Pasten-Zapata, E., Parra, R., Harter, T., Mahlknecht, J., 2014. Investigation of the geochemical evolution of groundwater under agricultural land: a case study in northeastern Mexico. J. Hydrol. 521, 410–423. https://doi.org/10.1016/j.jhydrol.2014.12.026.
Legates, D.R., McCabe, G.J., 1999. Evaluating the use of "goodness-of-fit" measures in hydrologic and hydroclimatic model validation. Water Resour. Res. 35 (1), 233–241.
McLean, W., Jankowski, J., Lavitt, N., 2000. Groundwater Quality and Sustainability in an Alluvial Aquifer, Australia Groundwater, Past Achievements and Future Challenges. A Balkema, Rotterdam, pp. 567–573.
Nematollahi, M.J., Ebrahimi, P., Razmara, M., et al., 2016. Hydrogeochemical investigations and groundwater quality assessment of Torbat-Zaveh plain, Khorasan Razavi, Iran. Environ. Monit. Assess. 188, 2. https://doi.org/10.1007/s10661-015-4968-6.
Parkhurst, D.L., Appelo, C.A.J., 2013. Description of Input and Examples for PHREEQC Version 3 - a Computer Program for Speciation, Batch-reaction, One-Dimensional Transport, and Inverse Geochemical Calculations: U.S. Geological Survey Techniques and Methods. book 6, chap. A43, 497 p., available only at. http://pubs.usgs.gov/tm/06/a43/.
Podgorski, J.E., Berg, M., 2020. Global threat of arsenic in groundwater. Science 368 (6493), 845–850. https://doi.org/10.1126/science.aba1510.
Polya, D.A., Middleton, D.R., 2017. Arsenic in drinking water: sources human exposure. In: Bhattacharya, P., Polya, D.A., Draganovic, D. (Eds.), Best Practice Guide on the Control of Arsenic in Drinking Water, 1st. International Water Association Publishing, London, UK. ISBN 9781843393856, Chapter 1.
Qasemi, M., Afsharnia, M., Farhang, M., Bakhshizadeh, A., Allahdadi, M., Zarei, A., 2018. Health risk assessment of nitrate exposure in groundwater of rural areas of Gonabad and Bajestan, Iran. Environ. Earth Sci. 77, 551.
Qasemi, M., Shams, M., Sajjadi, S.A., et al., 2019. Cadmium in groundwater consumed in the rural areas of Gonabad and Bajestan, Iran: occurrence and health risk assessment. Biol. Trace Elem. Res. 192, 106–115. https://doi.org/10.1007/s12011-019-1660-7.
Radfard, M., Yunesian, M., Nabizadeh, R., Biglari, H., Nazmara, Sh., Hadi, M., Yousefi, N., Yousefi, M., Abbasnia, A., Mahvi, A.H., 2019. Drinking water quality and arsenic health risk assessment in Sistan and Baluchestan, Southeastern Province, Iran. Hum. Ecol. Risk Assess. 25 (4), 949–965. https://doi.org/10.1080/10807039.2018.1458210.
Ravindra, K., Mor, S., 2019. Distribution and health risk assessment of arsenic and selected heavy metals in Groundwater of Chandigarh, India. Environ. Pollut. 250, 820–830.
Razavi Khorasan Management and Planning Organization, 2019. Spatial Planning Studies for Razavi Khorasan Province, Iran [In Farsi]. URL: https://khrazavi.mporg.ir/Portal/View/Page.aspx?PageId=6cd80675-0d18-43cc-9263-2ba794a490c1t=0 (Accessed: 23-Apr-2019).
Rezaei, A., Hassani, H., Hayati, M., et al., 2018. Risk assessment and ranking of heavy metals concentration in Iran's Rayen groundwater basin using linear assignment method. Stoch. Environ. Res. Risk Assess. 32, 1317–1336. https://doi.org/10.1007/s00477-017-1477-x.
Ricolfi, L., Barbieri, M., Muteto, P.V., et al., 2020. Potential toxic elements in groundwater and their health risk assessment in drinking water of Limpopo National Park, Gaza province, Southern Mozambique. Environ. Geochem. Health 42, 2733–2745. https://doi.org/10.1007/s10653-019-00507-z.
Sánchez-Martos, F., Pulido-Bosch, A., Molina-Sánchez, L., Vallejos-Izquierdo, A., 2002. Identification of the origin of salinization in groundwater using minor ions (Lower Andarax, Southeast Spain). Sci. Total Environ. 297 (1–3), 43–58. https://doi.org/10.1016/s0048-9697(01)01011-7.
Sepidbar, F., Mirnejad, H., Li, J.W., Wei, C., George, L.L., Burlinson, K., 2017. Mineral geochemistry of the Sangan skarn deposit, NE Iran: implication for the evolution of hydrothermal fluid. Geochemistry 77 (3), 399–419.
Shafaii Moghadam, H., Corfu, F., Chiaradia, M., Stern, R.J., Ghorbani, Gh., 2014. Sabzevar Ophiolite, NE Iran: progress from embryonic oceanic lithosphere into magmatic arc constrained by new isotopic and geochemical data. Lithos 210–211. https://doi.org/10.1016/j.lithos.2014.10.004.
Shojaat, B., Hassanipak, A.A., Mobasher, K., Ghazi, A.M., 2003. Petrology, geochemistry and tectonics of the Sabzevar Ophiolite, North Central Iran. J. Asian Earth Sci. 21 (9), 1053–1067. https://doi.org/10.1016/S1367-9120(02)00143-8.
Sohrabi, N., Kalantari, N., Amiri, V., et al., 2020. A probabilistic-deterministic analysis of human health risk related to the exposure to potentially toxic elements in groundwater of Urmia coastal aquifer (NW of Iran) with a special focus on arsenic speciation and temporal variation. Stoch. Environ. Res. Risk Assess. https://doi.org/10.1007/s00477-020-01934-6.
Statistical Center of Iran, 2019. Statistical Center of Iran [Online]. https://www.amar.org.ir/english. [Accessed: 23-Apr-2019].
Taghadosi, H., Malekzadeh Shafaroudi, A., 2018. Mineralogy, Alteration, geochemistry, and fluid inclusion studies of Fe oxide-copper mineralization of Namegh area, NE Kashmar. Iran. J. Crystallogr. Mineral. 26 (3), 541–554. https://doi.org/10.29252/ijcm.26.3.541.
Taheri, M., Mehrzad, J., Gharaie, M.H.M., Afshari, R., Dadsetan, A., Hami, S., 2016. High soil and groundwater arsenic levels induce high body arsenic loads, health risk and potential anemia for inhabitants of northeastern Iran. Environ. Geochem. Health 38 (2), 469–482.
Taherian, P., Joodavi, A., 2021. Hydrogeochemical characteristics and source identification of salinity in groundwater resources in an arid plain, northeast of Iran: implication for drinking and irrigation purposes. Acque Sotterranee - Italian J. Groundwater 10 (2), 21–31. https://doi.org/10.7343/as-2021-502.
Tahmasebi, P., Kamrava, S., Bai, T., Sahimi, M., 2020. Machine learning in geo- and environmental sciences: from small to large scale. Adv. Water Resour. 142, 103619 https://doi.org/10.1016/j.advwatres.2020.103619.
Tirkey, P., Bhattacharya, T., Chakraborty, S., Baraik, S., 2017. Assessment of groundwater quality and associated health risks: a case study of Ranchi city, Jharkhand, India. Groundw. Sustain. Dev. 5, 85–100. https://doi.org/10.1016/j.gsd.2017.05.002.
USEPA, 2020. Integrated Risk Information System (IRIS). Accessed date: 16 April 2020. http://www.epa.gov/iris/.
USEPA (US Environmental Protection Agency), 1999. A Risk Assessment-Multiway Exposure Spreadsheet Calculation Tool. United States Environmental Protection Agency, Washington D.C.
Vesali Naseh, M.R., Noori, R., Berndtsson, R., Adamowski, J., Sadatipour, E., 2018. Groundwater pollution sources apportionment in the Ghaen Plain, Iran. Int. J. Environ. Res. Public Health 15 (1), 172.
Wang, Y., Su, H., Gu, Y., Song, X., Zhao, J., 2017. Carcinogenicity of chromium and chemoprevention: a brief update. Onco. Ther. 10, 4065–4079. https://doi.org/10.2147/OTT.S139262.
World Health Organization-WHO, 2017. Guidelines for Drinking-Water Quality: Fourth Edition Incorporating the First Addendum. WHO, Geneva.
Wu, R., Podgorski, J., Berg, M., et al., 2020. Geostatistical model of the spatial distribution of arsenic in groundwaters in Gujarat State, India. Environ. Geochem. Health. https://doi.org/10.1007/s10653-020-00655-7.
Yousefi, M., Ghoochani, M., Mahvi, A.H., 2018. Health risk assessment to fluoride in drinking water of rural residents living in the Poldasht city, Northwest of Iran. Ecotoxicol. Environ. Saf. 148, 426–430. https://doi.org/10.1016/j.ecoenv.2017.10.057.
Zendehbad, M., Cepuder, P., Loiskandl, W., Stumpp, C., 2019. Source identification of nitrate contamination in the urban aquifer of Mashhad, Iran. J. Hydrol.: Regional Stud. 25, 100618 https://doi.org/10.1016/j.ejrh.2019.100618.
Zhou, P., Li, Z., Snowling, S., et al., 2019. A random forest model for inflow prediction at wastewater treatment plants. Stoch. Environ. Res. Risk Assess. 33, 1781–1792. https://doi.org/10.1007/s00477-019-01732-9.
Zirjanizadeh, S., Karimpour, M.H., 2016b. Mineralogy, geochemistry and petrography of intrusive volcanic rocks, Gonabad, Iran. Iran. J. Crystallogr. Mineral. 23 (4), 789–802. http://ijcm.ir/article-1-145-en.html.
Zirjanizadeh, S., Rocha, F., Santos, J.F., Samiee, S., 2016a. Origin of the Joumand fluorite and barite (Pb-Zn) veins of northwest Gonabad, Iran. Evidence from trace-element and stable (S) isotope data. Goldschmidt Conference Abstracts.